Mendeleev Communications

Focus Article, *Mendeleev Commun.*, 2027, **37**, in press

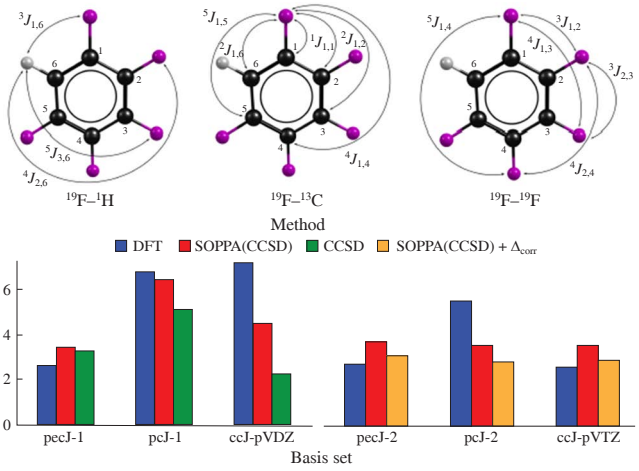
Computational methods in the NMR spectral analysis: from early semiempirical simulations to modern *ab initio* calculations

Leonid B. Krivdin

A. E. Favorsky Irkutsk Institute of Chemistry, Siberian Branch of the Russian Academy of Sciences, 664033 Irkutsk, Russian Federation. E-mail: krivdin55@gmail.com

DOI: 10.71267/mencom.8166

There are many hundreds, if not thousands of original publications and reviews dealing with different aspects of computational NMR applied to structural investigations of inorganic, organic, and bioorganic molecules together with organometallics and metal complexes. In the present review, we introduce a short overview of the most popular computational protocols – NMR simulations and semi-empirical calculations, DFT methods in NMR spectral analysis, and non-empirical NMR calculations. Several dozens of NMR simulative and iterative codes are used in the NMR spectral analysis. At the early stage of development of NMR computations, very popular were semiempirical methods based on complete or partial neglect of differential overlap. Later, the DFT NMR-based computations became very popular because they take into account electron correlation effects *via* the exchange–correlation potential requiring essentially low computational efforts. However, in the most recent years, NMR calculations are mostly performed based on general Polarization Propagator theory and Coupled Cluster methods. Of all these approaches, SOPPA(CCSD) and pure CCSD schemes turned out to be the most popular and robust methods for calculating NMR parameters.



Keywords: theoretical NMR, NMR simulations, computational methods, semiempirical calculations, structural elucidation, NMR spectral analysis, DFT methods, non-empirical NMR calculations.

1. Introduction

In continuation of the recent review[1] published in this journal by this author, briefly discussed in the present review, are recent advances in empirical NMR simulations, semiempirical and DFT NMR calculations, and *ab initio* calculations of chemical shifts and spin–spin coupling constants at different levels of non-empirical theory. These aspects are presented in much more detail in the recent reviews[2,3] and book chapter[4] by Rusakova and/or Krivdin.

2. NMR simulations and semiempirical calculations

There are dozens of NMR simulative and iterative codes – first of all those that were created for the iterative analysis of NMR strongly coupled spin systems, like classical LAOCOON, VALISA, and PANIC. A number of other less general codes like ANATOLIA, ANATOLIA-X, WinDNMR, NMR-SIM, DAISY, DAVINS, NMRCON, PERCHit, ChemAdder, NUTS, gNMR, MestRenova, SPINACH, SpinWorks together with



Leonid B. Krivdin graduated from M. V. Lomonosov Moscow State University in 1977 and received his PhD in 1982 from Irkutsk State University, followed by a postdoctoral fellowship at Flinders University of South Australia with Professor Ernst Della during 1990–1991. He received his DSc in 1989 and became a Full Professor in 1993. His research interests include the computational and theoretical interpretation of NMR parameters, supported by about 350 publications, including approximately 15 reviews and book chapters. Under his scientific supervision, 12 PhD and 2 DSc dissertations have been defended from 1989 to the present. Professor Krivdin has visited about 50 countries and has been invited as a visiting professor and/or lecturer at numerous universities and conferences worldwide. From 2007 to 2024, he served as Editor of *Magnetic Resonance in Chemistry*, a leading NMR journal. Leonid Krivdin is currently a Chief Researcher at the A. E. Favorsky Irkutsk Institute of Chemistry of the Russian Academy of Sciences and Chair of Chemistry at Angarsk State Technical University.

© 2027 Mendeleev Communications

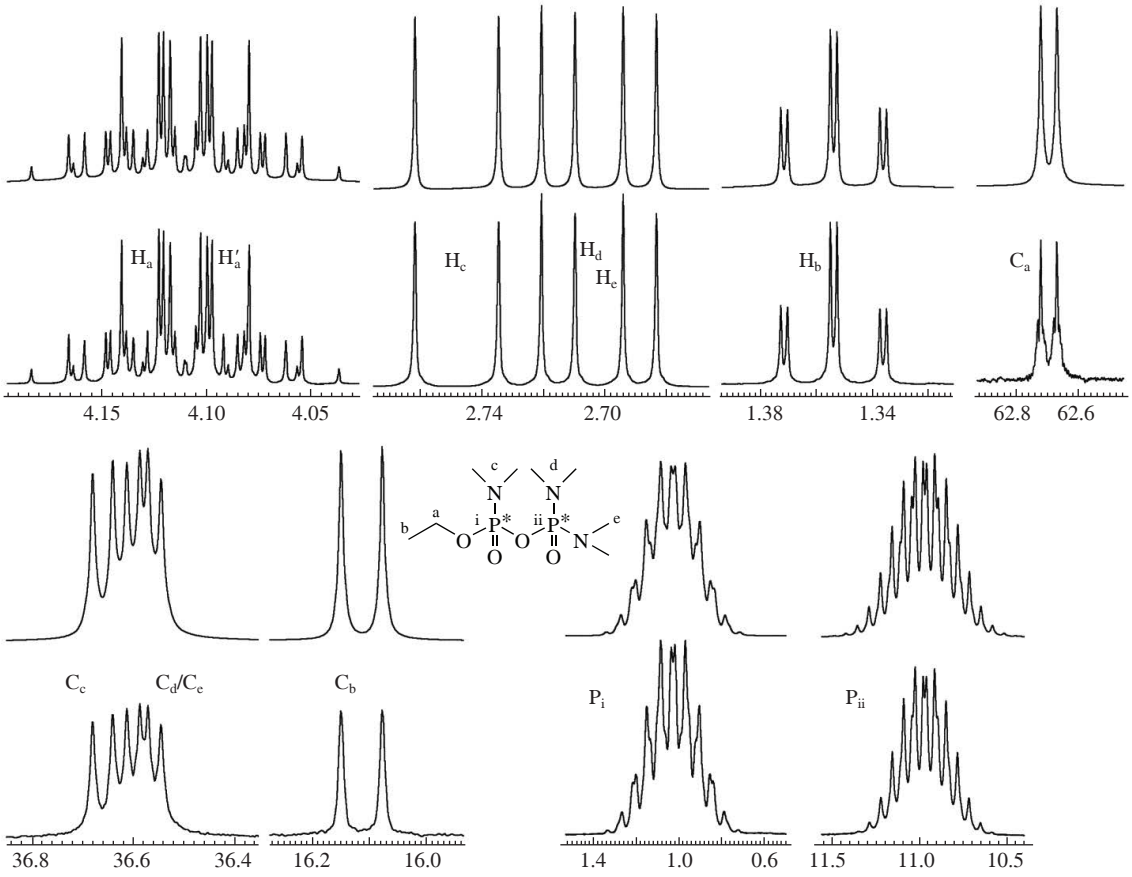


Figure 1 ^{1}H, $^{13}C\{^{1}H\}$, and ^{31}P NMR experimental spectra (below) as compared to the LAOCOON simulations (above) of a sample pyrophosphate – ethyl dimethylphosphoramidic tetramethylphosphoramidic anhydride (shown in figure). The asterisks mark the chiral atoms of phosphorus. Reproduced from Haapaniemi[5] with the permission of John Wiley & Sons, Inc.

many others were also established and were widely used in practice of NMR spectral analyses. All these programs are thoroughly reviewed.[2]

A nice example of LAOCOON analysis of a pyrophosphate reported by Haapaniemi[5] is presented in Figure 1. In this compound, all ^{1}H, $^{13}C\{^{1}H\}$ and ^{31}P NMR spectra are very complex due to the second-order coupling with phosphorus. As both magnetically nonequivalent ^{31}P nuclei are coupled to each other, the second-order coupling comes visible through all the resonances. This makes a structural elucidation very complicated, so that performing a full spectral analysis is necessary. All coupling constants available through the ^{1}H and ^{13}C NMR analysis were further verified with using them in simulation of the ^{31}P NMR spectra.

The ^{1}H resonances were identified based on their coupling patterns. The ^{1}H resonances of the methyl groups bound to nitrogen were assigned based on the large coupling to the nearby phosphorus. The coupling between *N*-methyl protons and phosphorus was found to be about 10.6 or 10.9 Hz. One dimethyl group was less shielded whereas the other two appeared more highfield. This information was in accordance with the molecular modeling results, where two nitrogen dimethyl groups were in a more crowded surroundings than the single dimethyl group near the *O*-ethyl group. The performed iterative analysis was fast and straightforward because final parameters did not significantly deviate from the input values. The assignment of ^{13}C resonances was also based on the chemical shift differences. Al *N*-methyl carbons resonated at around 36 ppm. One of them was less shielded and had larger coupling to phosphorus, thus suggesting belonging to one chiral phosphorus atom. The ethyl carbon adjacent to oxygen and methyl carbon at the end of the carbon chain resonated at around their characteristic areas, which finalized the identification of this compound performed mainly with LAOCOON.

As an illustration of the efficiency of the strongly coupled spin system iterative simulation, early results by Zubkov *et al.*[6] could also be mentioned. The authors proposed a new strategy of the total lineshape analysis of the multiplet structure of NMR spectra by means of a VALISA program developed to implement original computational procedure. Using a complete set of vicinal spin–spin coupling constants, a detailed conformational analysis of *trans*-1,2-dibromocyclopentane was carried out and a more correct model for the description of conformational interconversions of the five-membered cycles was proposed. Conformational behavior of *trans*-1,2-dibromocyclopentane was reasonably described assuming large amplitude molecular vibrations along a sector of the pseudorotation path.

In the case of VALISA program, white noise was added to the spectrum of pyridine with the levels of 2.5, 10, and 40% of the amplitude of the most intense signal.[6] The halfwidth of each spectral line was 0.36 Hz and an additional line broadening of 3, 1, and 0.5 Hz was used during the iterative process. As can be seen in Figure 2, even at very high level of noise in the spectrum the iterative process overcomes numerous noise-induced local minima and finds a rather correct solution. This was possible owing to substantial improvement of the effective signal-to-noise ratio in the intermediate (broadened) spectra at the cost of a loss of resolution. In fact, the broadening procedure used by VALISA represented a commonly accepted noise reduction technique used in routine NMR spectra. It was thus demonstrated that a small additional broadening of spectral components caused no loss of information on the multiplicity of the system under study.

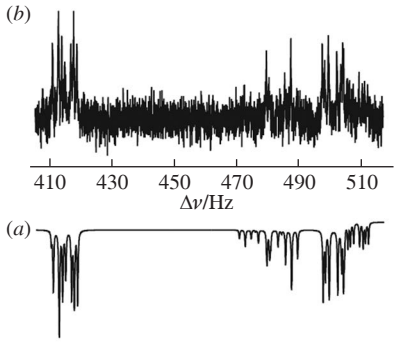


Figure 2 ^{1}H NMR spectrum of pyridine in solution (*a*) that with the highest signal-to-noise ratio and (*b*) that obtained with the highest noise level, both simulated by the VALISA program. Reproduced with minor editing privilege from Zubkov *et al.*[6] under the CC BY-NC 4.0 International Public License.

Much more recently, the more robust program code acronymed as ANATOLIA[7] has appeared. This open-source software code was created for the total lineshape analysis of NMR spectra by the fitting of experimental 1D NMR spectra based on quantum mechanical formalism. The main purpose of ANATOLIA was an accurate determination of spin–spin coupling constants and elucidation of complicated multiplet structures including strongly coupled systems, as illustrated in Figure 3. It utilized the Lorentzian broadening approach for the local minima suppression and was developed in the C++ language for the standard personal computers.

Generally, ANATOLIA was also shown in those papers to be able to yield accurate spectral parameters from inaccurate input values. ANATOLIA software has been thoroughly tested on pentafluorobenzene and tetrafluoro-4-(morpholino)pyridine[8] and further on for the complex ^{1}H, ^{19}F, and ^{13}C multiplets of two biologically active compounds.[9] The latter were produced as part of a family of fluorinated drug scaffolds prepared for anticancer and antiparasitic screening. A spin-system of six coupling nuclei (four protons and two fluorines) was analyzed in 12 s, a spin-system of nine coupled fluorine nuclei was analyzed within

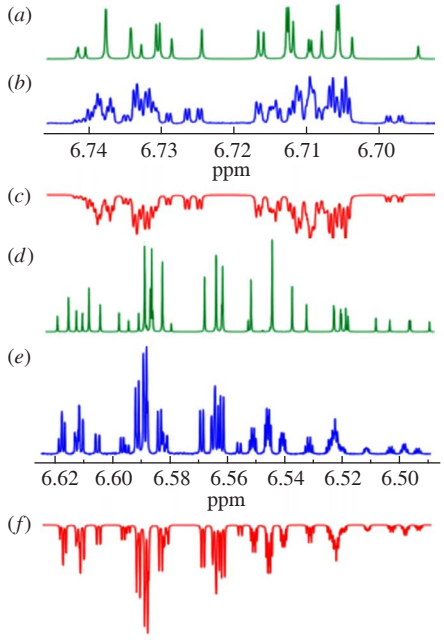
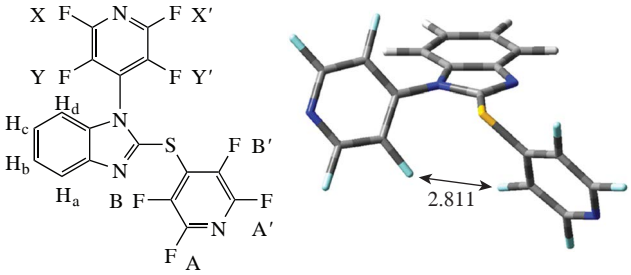


Figure 3 Comparison of (*a*, *d*) ANATOLIA theoretical spectrum of styrene with initial parameters, (*b*, *e*) experimental spectrum, and (*c*, *f*) resulted ANATOLIA theoretical spectrum after refinement of *J*-couplings. The region of aromatic protons is shown (300 MHz, 303 K, 0.5 M in benzene-d_6). Reproduced with minor editing privilege from Cheshkov *et al.*[7] with the permission of John Wiley & Sons, Inc.

2 min, and 10 coupled nuclei was optimized in 6 min using a laptop computer. This is illustrated in Figures 4–6 showing ANATOLIA spectral analysis of strongly coupled ^{1}H, ^{13}C, and ^{19}F NMR spectra of 1-tetrafluoropyrid-4-yl-2-tetrafluoropyrid-4-ylthio-1*H*-benzimidazole:



In a very recent publication by Nichugovskiy *et al.*,[10] two novel tools, namely the First-Order Multiplet Analyzer (FOMA) and ANATOLIA with X-factorization (ANATOLIA-X), were introduced. FOMA is a first-order multiplet analyzer designed for the total lineshape fitting of a single strongly coupled first-order multiplets, while ANATOLIA-X is a modified version of the program ANATOLIA complemented with X-factorization of spin Hamiltonian, the latter allowing for the analysis of individual strongly coupled multiplets.

To validate the FOMA performance, authors successfully analyzed a very strongly coupled multiplet of the menthol's H-5 proton. On the other hand, further validation of FOMA software was performed on the strongly coupled ^{119}Sn multiplet of trimethyl (perfluorophenyl)stannane where FOMA unambiguously generated theoretical spectrum that closely matched the experimental multiplet structure. In both cases, the program successfully parsed the multiplet pattern, manifesting excellent agreement between theoretical simulation and experiment, as illustrated in Figure 7.

As can be seen in Figure 8, the ^{1}H NMR spectrum of the vinylnorbornene dissolved in deuterated chloroform exhibits

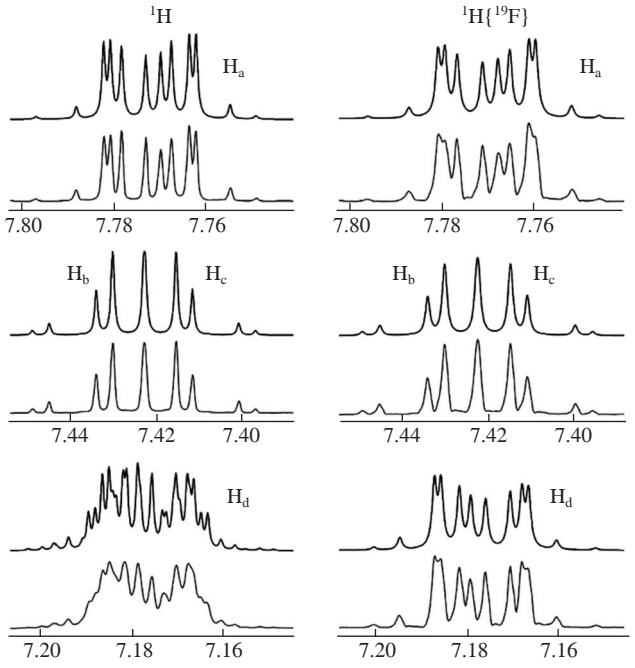


Figure 4 Experimental (lower) and ANATOLIA calculated (upper) ^{1}H NMR multiplets of 1-tetrafluoropyrid-4-yl-2-tetrafluoropyrid-4-ylthio-1*H*-benzimidazole, ~20 mg in 0.7 ml of $CDCl_3$ referenced to tetramethylsilane at 0.0 ppm. ^{1}H (left), and ^{1}H{sel-dec-^{19}F} (right) spectra recorded using a JEOL ECZ 500. Reproduced from Edgar *et al.*[9] with the permission of John Wiley & Sons, Inc.

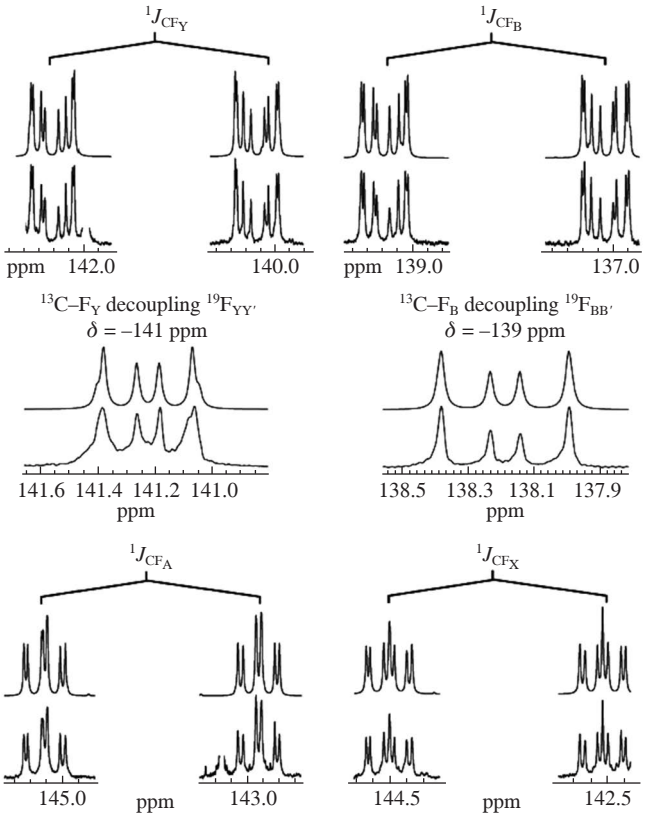


Figure 5 Experimental $^{13}C\{^1H\}$ NMR spectra (lower) and calculated (upper) of 1-tetrafluoropyrid-4-yl-2-tetrafluoropyrid-4-ylthio-1*H*-benzimidazole, ~20 mg in 0.7 ml of $CDCl_3$ recorded using a JEOL ECZ 500. Experimental $^{13}C\{sel\text{-}^{19}F\}$ NMR spectra (lower) and calculated (upper) removed the large $^1J_{CF}$ coupling and the associated $^3J_{CF}$ couplings and produced the much simplified ^{13}C multiplet and reduced the spin-systems to ^{13}C-YY′ and ^{13}C-BB′ comprising of $^2J_{CF}$, $^4J_{CF}$ coupling constants only. Reproduced from Edgar *et al.*[9] with the permission of John Wiley & Sons, Inc.

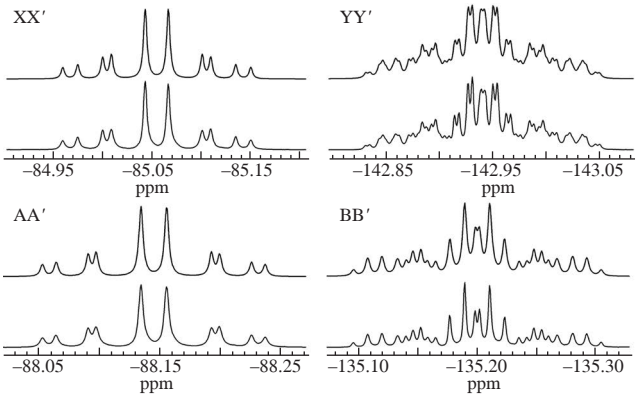


Figure 6 Experimental ^{19}F NMR spectra (lower) and calculated (upper) of 1-tetrafluoropyrid-4-yl-2-tetrafluoropyrid-4-ylthio-1*H*-benzimidazole, analyzed using data derived from *ab initio* calculations, which was then further optimized using ANATOLIA, ~20 mg in 0.7 ml of $CDCl_3$ referenced $CFCl_3$ = 0 ppm, recorded using a JEOL ECZ 500. Reproduced from Edgar *et al.*[9] with the permission of John Wiley & Sons, Inc.

significant signal overlap, particularly that for the bridgehead protons, which provides very close chemical shifts regardless of the orientation of the vinyl group. The ^1H NMR signals of its major isomer display a first-order spectrum, with the difference in resonance frequencies significantly exceeding coupling constants for all coupled proton pairs. In contrast, the minor isomer provides complex multiplet patterns due to small frequency differences between four methylene protons. To obtain accurate values of those spin-system parameters (^1H NMR chemical shifts and ^1H–^1H spin–spin coupling constants) for both isomers, it was necessary to perform a total lineshape analysis of their ^1H NMR spectra, as illustrated in Figures 9 and 10. Fitting the spectrum of the 12-spin system without any approximations required nonlinear optimization of as many as 78 parameters, which illustrates the benefits of ANATOLIA-X.

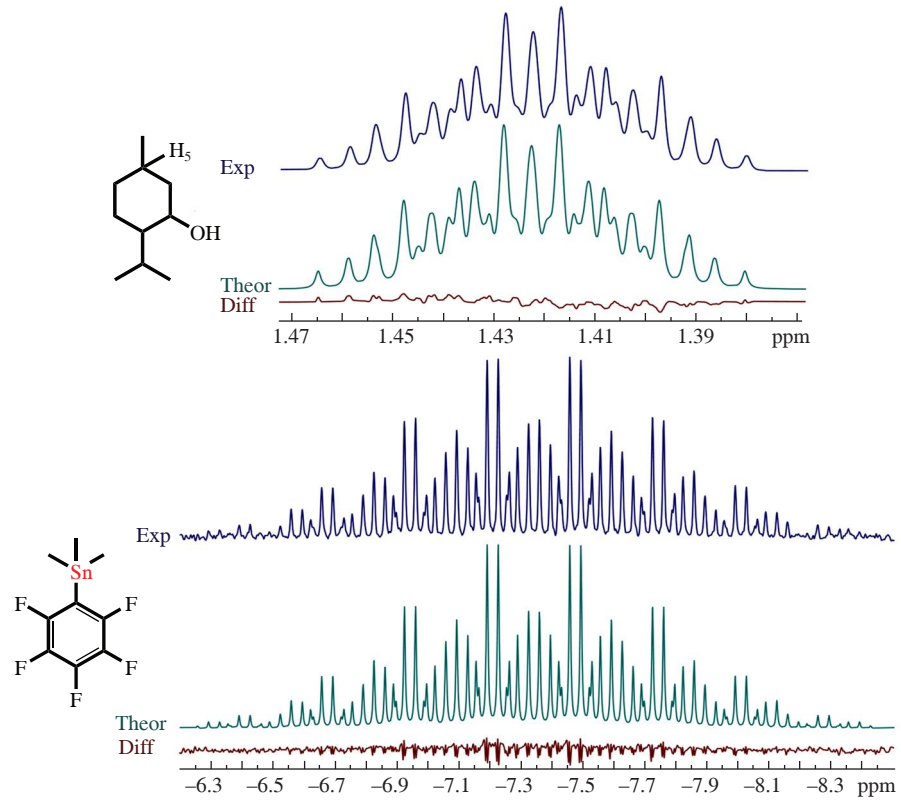


Figure 7 Application of FOMA to the analysis of complicated first-order multiplets: top – multiplet of menthol proton H-5 (600.13 MHz, 0.5 M in $CDCl_3$, 300 K); bottom – ^{119}Sn multiplet of $C_6F_5SnMe_3$ (223.86 MHz, 0.5 M in CH_2Cl_2, external D_2O LOCK, 295.5 K). Reproduced from Nichugovskiy *et al.*[10] with the permission of John Wiley & Sons, Inc.

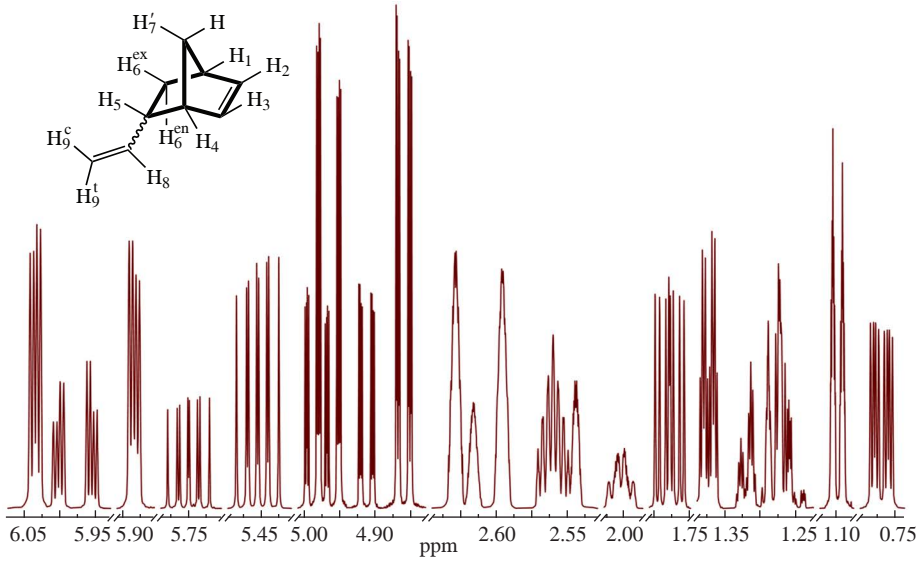


Figure 8 Vinylnorbornene chemical structure, atom numbering, and ^{1}H NMR spectrum overview (600.03 MHz, 1 M in C_6D_6, 303 K). Reproduced from Nichugovskiy *et al.*[10] with the permission of John Wiley & Sons, Inc.

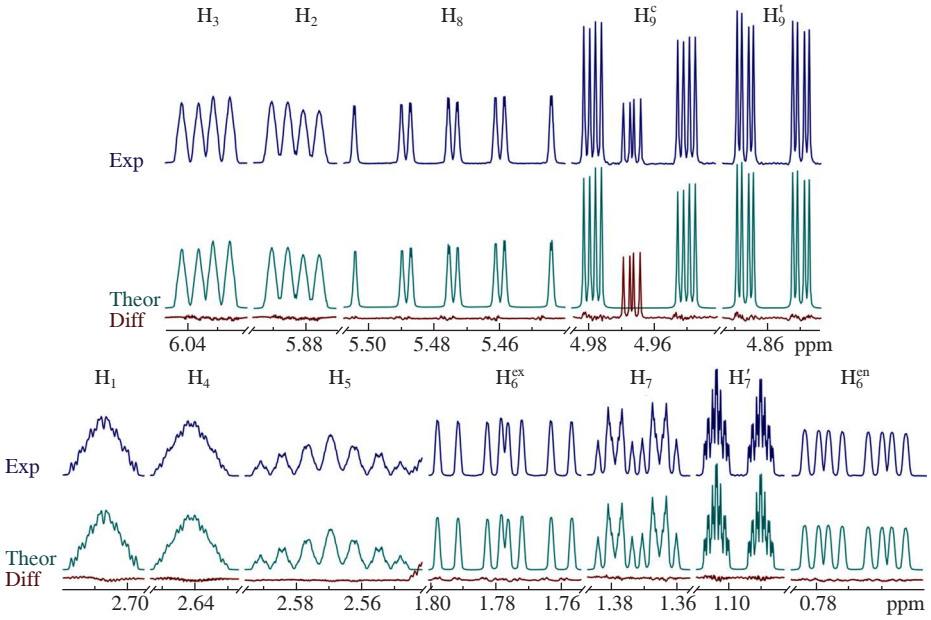


Figure 9 Results of the ^{1}H spectrum total lineshape fitting using ANATOLIA-X of the major vinylnorbornene isomer (600.03 MHz, 0.6 M in C_6D_6, 303 K). Reproduced from Nichugovskiy *et al.*[10] with the permission of John Wiley & Sons, Inc.

In the second more theoretical recent paper by Cheshkov and Sinitsyn[11] dealing with the high-accuracy ANATOLIA-based spectral analysis of the strongly-coupled spin systems, authors established a connection between the symmetry of the high-order NMR spectra and the properties of the corresponding spin system. It was shown that for a spectrum to be symmetric about the mid-resonance frequency ν_0, two conditions must be satisfied: (*a*) the resonance frequencies of the spins must be symmetrically positioned about ν_0, and (*b*) there should exist at least one spin ordering with a monotonic increase (or decrease) in the resonance frequencies. Under second condition, the spectrum is invariant under the reflection of the *J*-coupling matrix about its anti-diagonal. Those theoretical results were validated by theoretical spectra for the four-, five-, and six-spin systems with particular values of ν and *J*, as exemplified in Figure 11.

PANIC (Parameter Adjustment in NMR by Iteration Calculation) code is a minicomputer version of the LAOCOON type programs used on large computer systems. Utilizing PANIC, nuclear spin systems of up to eight magnetically inequivalent nuclei may be calculated. The spectral parameters defining the system not only evaluates chemical shifts and scalar spin–spin coupling constants, but also provides direct dipole–dipole coupling constants, observable in the axially oriented spin systems, and quadrupole coupling constants for nuclei with spins larger than one half. In addition, PANIC includes the weak coupling algorithm, a technique for handling magnetic equivalence and error estimates for the adjusted parameters. PANIC code was written on ASPECT Assembler Language for BRUKER spectrometers. Since ASPECT computers are out of production for many years, PANIC is no longer maintained. The performance of PANIC in the high-precision iterative analysis of ^{1}H and proton-coupled ^{13}C NMR spectra of individual molecules is illustrated in Figures 12–16 adopted from the early reference.[12]

Nowadays, different NMR simulative programs are used routinely by chemists mainly for getting instantaneous results of spectral analysis without going into details of the performed simulations.

It should be recalled that on the early stage of NMR computations, very popular were a family of semiempirical methods involving CNDO (Complete Neglect of Differential

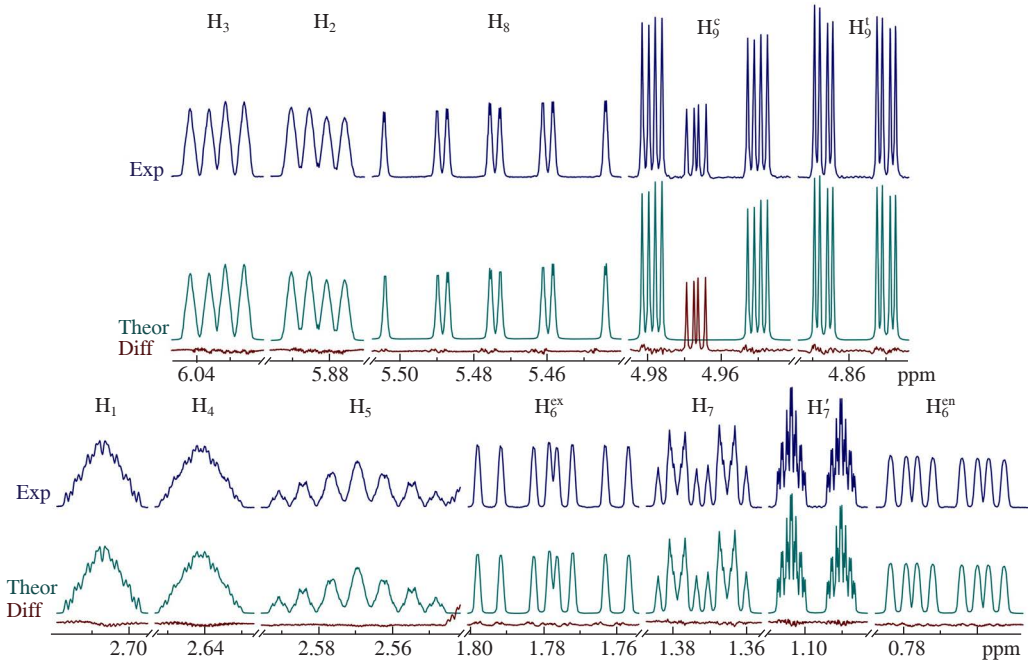


Figure 10 Results of the ^{1}H spectrum total lineshape fitting using ANATOLIA-X of the minor vinylnorbornene isomer (600.03 MHz, 0.6 M in C_6D_6, 303 K). Reproduced from Nichugovskiy *et al.*[10] with the permission of John Wiley & Sons, Inc.

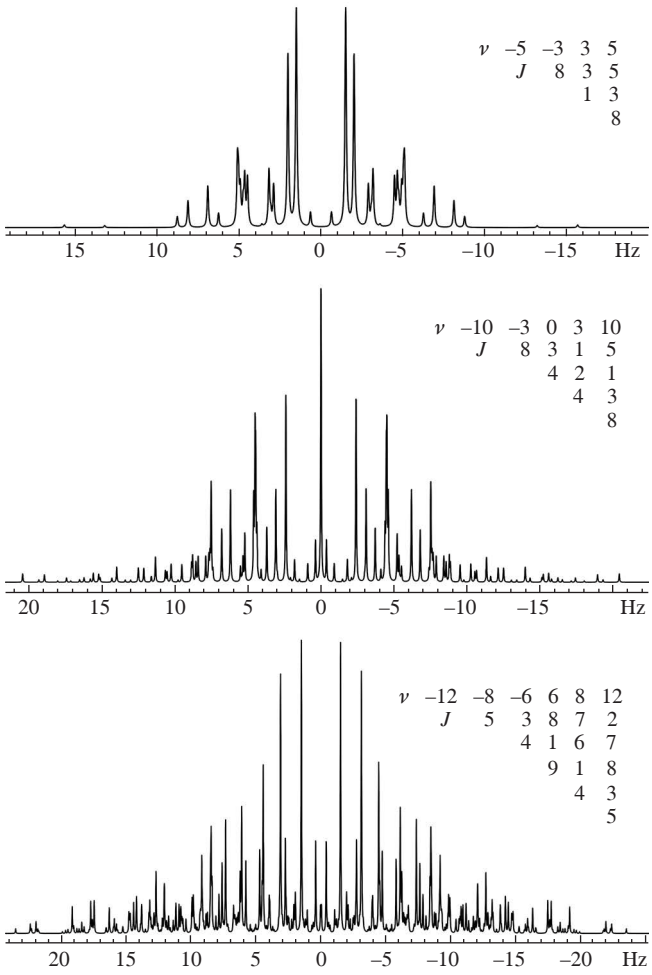


Figure 11 Theoretical mirror-symmetric spectra for the four (top), five (middle), and six (bottom) spin systems with specific values of ν and J. Reproduced from Cheshkov and Sinitsyn[11] under the CC BY-NC 4.0 International Public License.

Overlap),[13] INDO (Intermediate Neglect of Differential Overlap),[14] MINDO (Modified Intermediate Neglect of Differential Overlap),[15] MNDO (Modified Neglect of Diatomic

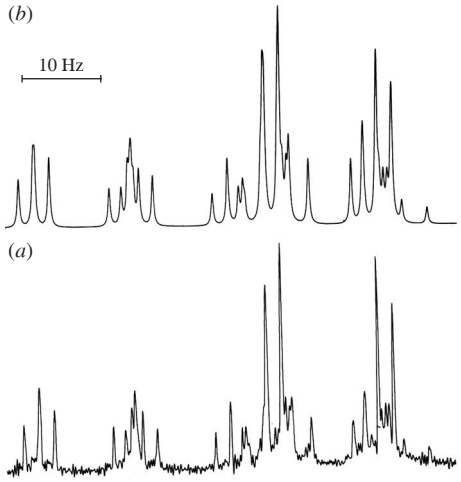


Figure 12 (*a*) ^{1}H NMR spectrum of *o*- and *p*-aromatic protons of *tert*-butoxybenzene in $CDCl_3$ (degased sample in a sealed 5 mm tube) recorded at 100 MHz on a Varian XL-100 spectrometer. (*b*) The same spectrum simulated with PANIC (Lorenz lines, halfwidths 0.2 Hz). Reproduced from ref. 12 with the permission of the author.

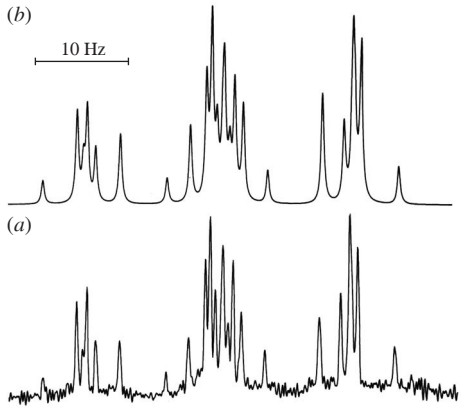


Figure 13 (*a*) ^{1}H NMR spectrum of *m*-aromatic protons of *tert*-butoxybenzene in $CDCl_3$ (degased sample in a sealed 5 mm tube) recorded at 100 MHz on a Varian XL-100 spectrometer. (*b*) The same spectrum simulated with PANIC (Lorenz lines, halfwidths 0.2 Hz). Reproduced from ref. 12 with the permission of the author.

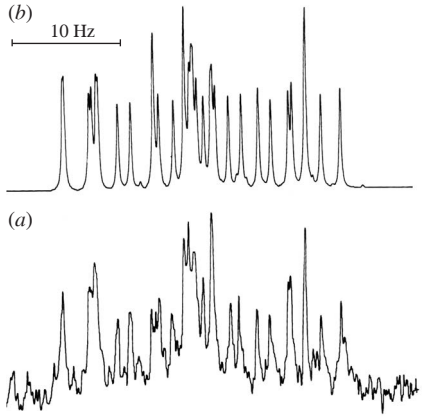


Figure 14 (*a*) Proton-coupled ^{13}C NMR spectrum of *ipso*-isotopomer of *tert*-butoxybenzene in $CDCl_3$ (degased sample in a sealed 10 mm tube) recorded at 25 MHz on a Varian XL-100 spectrometer. (*b*) The same spectrum simulated with PANIC (Lorenz lines, halfwidths 0.2 Hz). Reproduced from ref. 12 with the permission of the author.

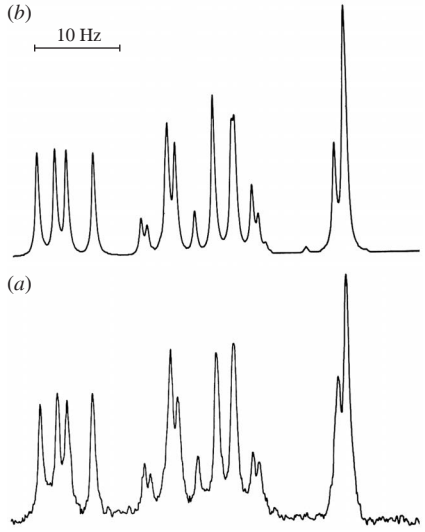


Figure 15 (*a*) Highfield multiplet of the proton-coupled ^{13}C NMR spectrum of *ortho*-isotopomer of *tert*-butoxybenzene in $CDCl_3$ (degased sample in a sealed 10 mm tube) recorded at 25 MHz on a Varian XL-100 spectrometer. (*b*) The same spectrum simulated with PANIC (Lorenz lines, halfwidths 0.2 Hz). Reproduced from ref. 12 with the permission of the author.

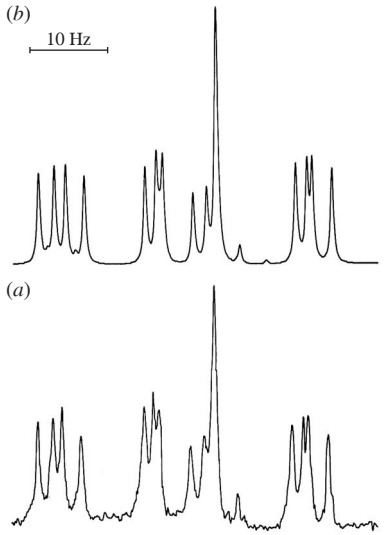


Figure 16 (*a*) Lowfield multiplet of the proton-coupled ^{13}C NMR spectrum of *ortho*-isotopomer of *tert*-butoxybenzene in $CDCl_3$ (degased sample in a sealed 10 mm tube) recorded at 25 MHz on a Varian XL-100 spectrometer. (*b*) The same spectrum simulated with PANIC (Lorenz lines, halfwidths 0.2 Hz). Reproduced from ref. 12 with the permission of the author.

Overlap),[16] AM1 (Austin Model 1),[17] and PM3 (Parameterized Model 3).[18] Herewith we will not go into details of those methods and provide here no references, which is because they represent only historical interest.

Very briefly, CNDO simplifies calculations by approximating that the overlap between different atomic orbitals is zero. Developed by John Pople and collaborators, it was one of the first methods, which used two main approximations: the 'core approximation' (only outer valence electrons are explicitly calculated) and the zero-differential overlap approximation. INDO method is a development of CNDO and allows for efficient calculations, especially of excited states in large organic molecules, by making specific approximations in the calculations. MINDO was developed by the group of Michael Dewar. This method should actually be referred to as MINDO/3. It was later replaced by the MNDO method, which in turn was replaced by the AM1 and PM3 methods. AM1 simplifies the Schrödinger equation by using experimental parameters, which makes it faster while still providing accurate results for many applications like geometry optimizations. Developed by Michael Dewar, AM1 is actually a refinement of the older MNDO method. In the PM3 method, the reduction of two-center repulsive forces is brought about by the parameterization of the Gaussian core–core interactions. It predicts electronic properties and geometric parameters, showing some obvious advantages over other methods like most popular in those days AM1. The other differences lie in the philosophy and the methodology used during the parameterization: AM1 takes some of the parameter values from spectroscopic measurements whereas PM3 treats them as optimized values.

3. DFT calculations

The DFT method has become extremely popular in recent years because it takes into account electron correlation effects *via* the exchange–correlation potential, while having very moderate computational requirements. Indeed, the formal scaling of the computing time for the DFT method is comparable with that of the Hartree–Fock method, being only of $O(N^4)$ (with N representing the size of the basis set functional space). The main idea of the density functional theory consists in using the electron density rather than a many-particle wavefunction for describing a given electron system. This leads to a significant simplification of the problem in view of computational requirements because the many-particle wavefunction depends on $3M$ variables, where M is the number of electrons. At that, the electron density represents a function of only three spatial coordinates.

Modern applications of the DFT theory to the calculation of NMR chemical shifts have been developed by Malkin *et al.*[19–21] based on the Individual Gauge for Localized Orbitals (IGLO) method[22] and by Schreckenbach and Ziegler[23–27] who used the Gauge-Including Atomic Orbitals (GIAO) approach.[28–31] A number of other implementations of DFT theory for NMR shielding constants, mostly those based on the GIAO method, have also been presented within the same period of time.[32,33]

There were a number of efforts to bypass numerous problems connected with applying different DFT functionals.[34,35] In this context, appeared recently was a special area of research aimed at the enhancement of the performance of the DFT method applied to the calculation of nuclear magnetic shielding constants. First attempts were directed to the introduction of some principal corrections[20,36,37] which followed by the creation of hybrid functionals with a constant exact-exchange (EXX) admixture[31,38] or explicit empirical parametrization of semi-local functionals for shielding constants and chemical shifts.[39,40]

In some cases, the global hybrids and parametrized functionals like KT1, KT2, and KT3 can improve the performance of the

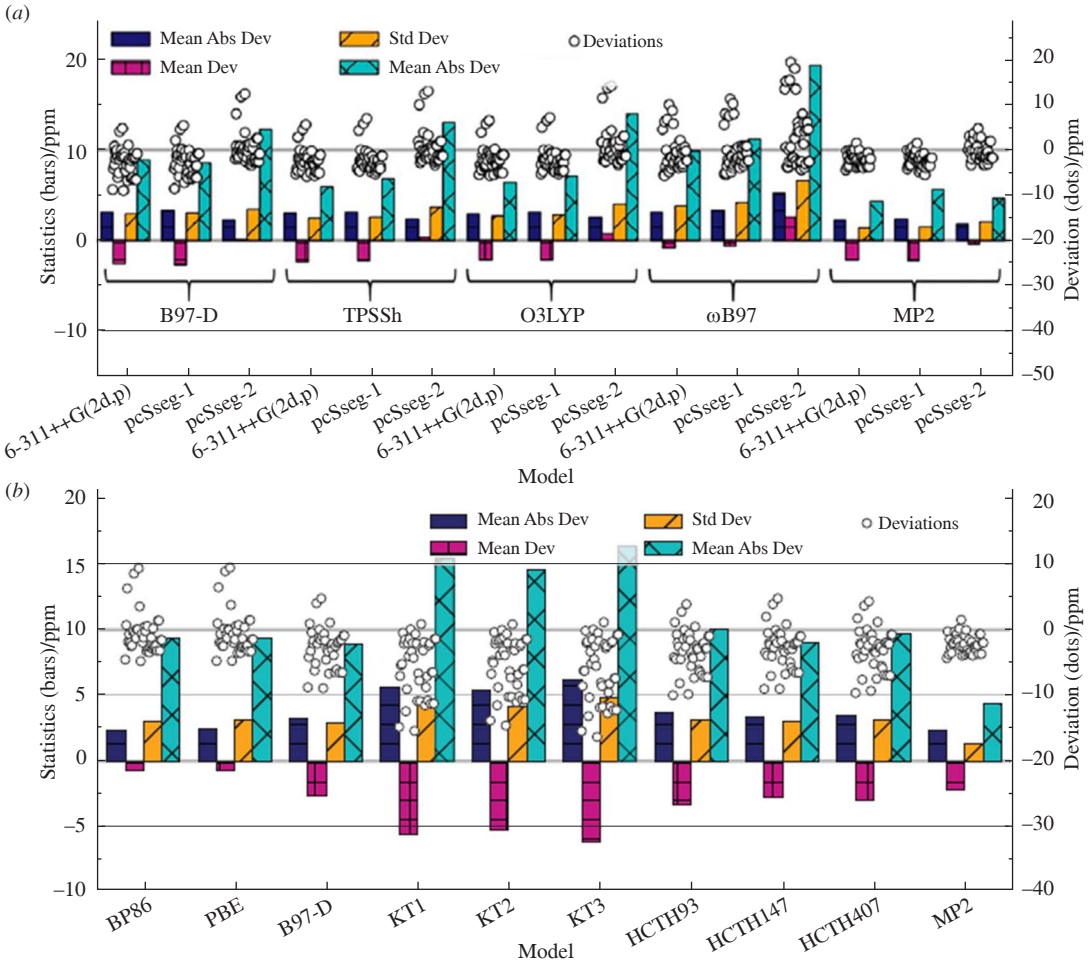


Figure 17 Performance of different basis sets (*a*) and GGA functionals (*b*) *versus* experiment. Reproduced with minor editing privilege from Zhan *et al.*[41] with the permission of John Wiley & Sons, Inc.

DFT method for shielding constants as compared to the semi-local functionals, but in general, the improvement of accuracy can be very limited or even absent, as can be seen, for example, from the bottom diagram in Figure 17. Long-range corrected functionals provide a somewhat better performance of the DFT method towards the linear-response properties such as NMR shielding constants as compared to usual GGA functionals, which was explicitly demonstrated by Zahn *et al.*[41] for proton and carbon chemical shifts. However, notwithstanding the fact that the range-separated functionals are particularly popular today, they still do not provide notable improvement, and the exploration of the other possible ways of increasing the accuracy of DFT method applied to the NMR calculations is widespread nowadays.

One of the modern findings in this field is the creation of the double hybrid functionals.[42] They do give very precise results for NMR shielding constants as compared to the CCSD(T) benchmark data, though they contain a fraction of the MP2 correlation. As a result, if applied in combination with large basis sets and GIAO formalism, their computational advantage significantly decreases, which is because NMR calculations carried out with such functionals become computationally very demanding, which drastically limits their practical usage.

Saielli reported the results of the DFT study of the one-bond $^{1}J(^{15}N,^{19}F)$ spin–spin coupling constants in a series of fluorinating reagents containing N–F bond.[43] The results of the those calculations performed at the M06-2X(PCM)/pcJ-2//B3LYP/6-311G(d,p) level provided very good linear relationship with the experimental values, which was characterized by a MAE of about 5 Hz, see Figure 18. Those calculations allowed to analyze molecular orbital contributions to the studied spin–spin coupling constants, as illustrated in Figure 19, and to rationalize observed positive sign corresponding to a negative sign of the reduced spin–spin coupling constants between nitrogen and fluorine. Spin–dipolar and paramagnetic spin–orbital contributions were found to account for about 60% of the Fermi contact term. Orbital contributions to those spin–spin coupling constants showed a complex electronic pattern, which was responsible for the negative sign of the reduced one-bond $^{15}N–^{19}F$ coupling constants and therefore for the positive sign of $^{1}J(^{15}N,^{19}F)$ coupling constants. Also, calculated coupling constants provided a very good correlation with the N–F bond lengths.

Reviriego and colleagues[44] reported a DFT study of 10-hydrazino-BODIPY, $BoNHNH_2$, using traditional B3LYP functional in combination with the traditional Pople's 6-311G(d,p) basis set. This BODIPY provided slow rotation around the C10–NH bond resulting in 'anisochronous' ^{1}H and ^{13}C NMR signals. The assignment of NMR signals was performed using traditional two-dimensional methods and confirmed by the DFT calculations. Based on those results, six C–H protons of $BoNHNH_2$ have been reduced to one out of 720 (!) possible combinations. Additionally, the rotational barrier has been determined in three pairs of proton signals and compared with the calculated one. Results of that study are summarized in Figure 20.

A series of NMR-oriented basis sets for calculation of chemical shifts and spin–spin coupling constants were created recently. As an example, Provasi and Sauer with colleagues presented the coupling constants-oriented basis sets aug-cc-

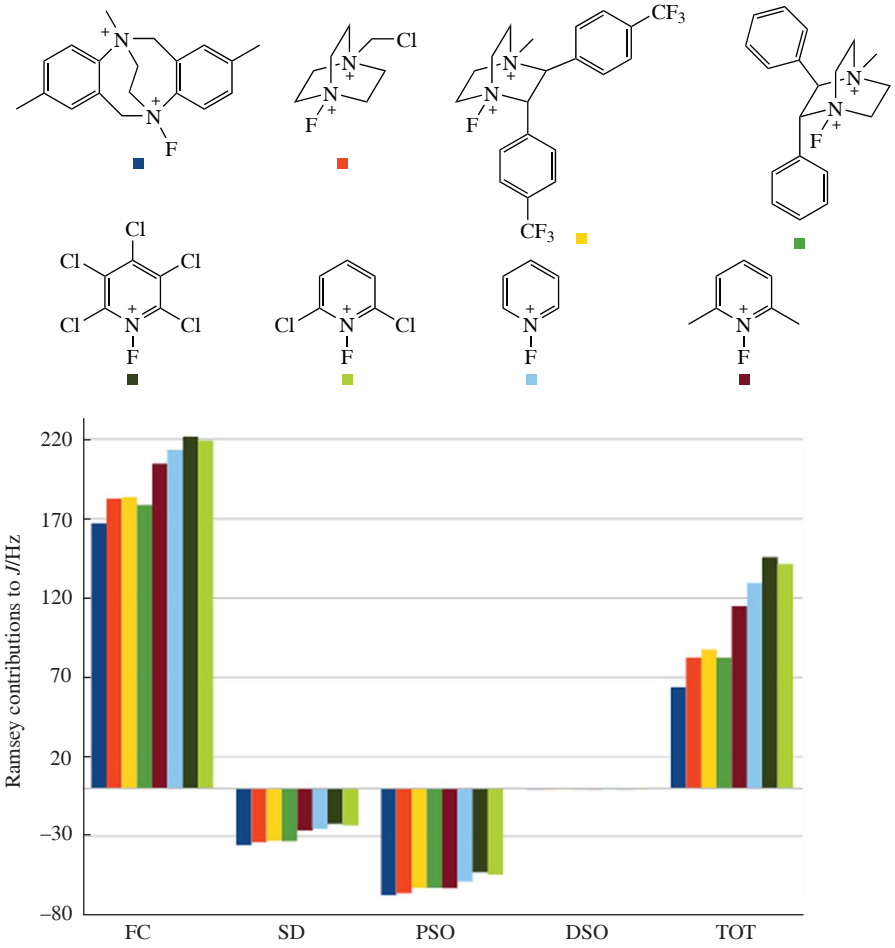


Figure 18 Ramsey contributions to the total $^{1}J(^{15}N,^{19}F)$ spin–spin coupling constants calculated at the M06-2X(PCM)/pcJ-2//B3LYP(PCM)/6-311G(d,p) level. Reproduced with minor editing privilege from Saielli[43] with the permission of Wiley.

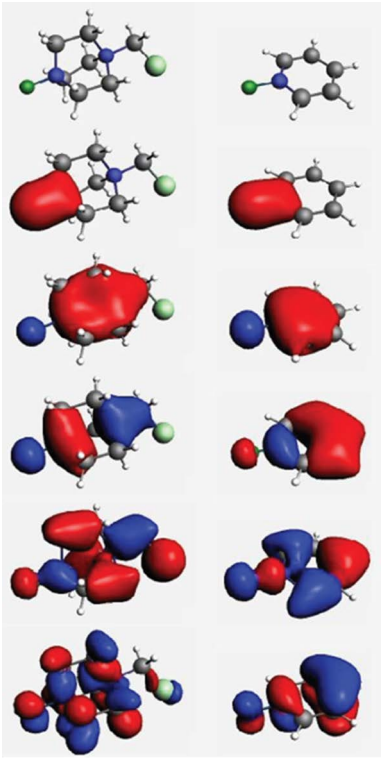


Figure 19 Occupied molecular orbitals giving the largest contribution to the $J(^{15}N,^{19}F)$ spin–spin coupling constants. Top: molecular geometry; left: 1-(chloromethyl)-4-fluoro-1,4-diazabicyclo[2.2.2]octane-1,4-diium; right: 1-fluoropyridin-1-ium. Reproduced with minor editing privilege from Saielli[43] with the permission of John Wiley & Sons, Inc.

pVTZ-J for H, C, and O,[45,46] B, Al,[45,47] F,[45,48] Si,[47,49,50] P, Cl,[47] S,[46] Sc–Zn,[51] Ga, Ge, As, Se, and Br.[52] These basis sets were created based on the sequential even-tempered saturation of the basis set shells in the important regions.

The other group of coupling constants-oriented basis sets is that of Jensen, (aug)pcJ-*n* ($n = 0$–4),[53–55] which are suitable for the calculation of spin–spin coupling constants for the 1–3 row elements (H–Ar) with the density functional methods and applicable for rather large molecular systems at a favorable computational cost. Jensen's basis sets were developed on the grounds of previously proposed series of the energy-optimized polarization-consistent basis sets (aug)pc-*n* ($n = 0$–4)[56–60] by augmenting them with tight *s*-, *p*-, *d*-, and *f*-functions and determining the additional optimum exponents with a variational procedure for the sum of the absolute values of all four contributions.

Other coupling constants-oriented basis sets were created by Rusakov and Rusakova, namely, the acvXz-J (X = 2, 3, 4) for Se, Te,[61] and Sn[62] using even-tempered saturation approach, and, most recently, the pecJ-*n* ($n = 1, 2$) for H, C, N, F,[63] P, Si,[64] and Se[65] based on the property-energy consistent (PEC) method.[63]

Specialized coupling constants-oriented basis sets usually reflect the peculiarities of spin–spin coupling constants, which follow from the simplest nonrelativistic Ramsey's formulation of that property as the sum of four different contributions – the Fermi contact (FC), the spin dipolar (SD), the paramagnetic spin–orbit (PSO), and the diamagnetic spin–orbit (DSO) terms. The FC term was found to primarily depend on the electron density at the nuclear position and, for the proper description, requires tight *s*-type functions, expressed with very high exponents. The PSO and SD terms involve hyperfine operators

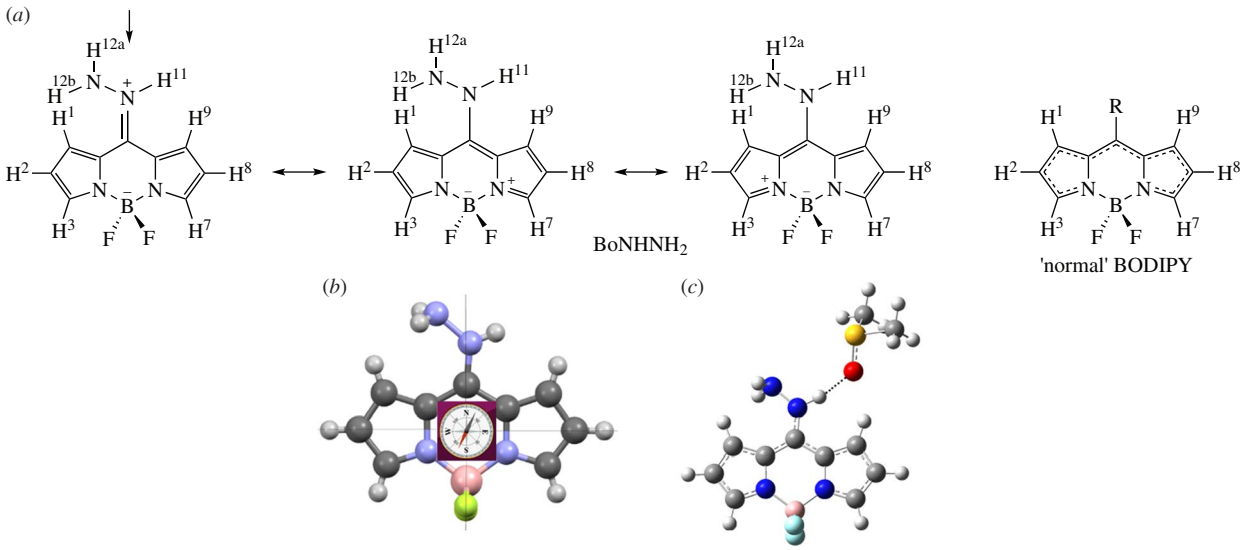


Figure 20 (*a*) The resonance forms and delocalization of $BoNHNH_2$ together with a 'normal' BODIPY; (*b*) the 'compass' geometry of $BoNHNH_2$; (*c*) structure of the $BoNHNH_2$···DMSO complex linked by the N–H···O hydrogen bond. Reproduced with minor editing privilege from Reviriego *et al.*[44] with the permission of John Wiley & Sons, Inc.

that primarily concern the inner region of the wave function. The DSO term is usually very small; hence, it is not paid much attention in this respect.

Specialized basis sets for NMR shielding constants are much too scarce. One series comprises Jensen's pcS-*n* (*n* = 0–4) basis sets for the elements of the 1–3 periods (H–Ar) and pcSseg-*n* (*n* = 0–4) basis sets[66] for the elements of the 1–4 periods (H–Kr). The other series includes error-consistent segmented contracted all-electron relativistic basis sets for elements from hydrogen to radon by Franzke *et al.*,[67] namely, the x2c-SVPall-s, x2c-TZVPall-s, x2c-TZVPPall-s, x2c-QZVPall-s, x2c-QZVPall-2c-s, x2c-QZVPPall-s, and x2c-QZVPPall-2c-s basis sets. The most recent series includes Rusakov's basis sets, namely, the (aug-)pecS-*n* (*n* = 1, 2) for H, C, N, O[68–70] and P atoms.[71,72] The PEC method is rapidly developing right now, and as an example, the equilibrium geometry-oriented basis sets, pecG-*n* (*n* = 1, 2), were presented in 2024; the latter were shown to reduce to minimum the error connected with the geometry factor in the calculations of NMR shielding constants.[73–75]

It should be emphasized that all specialized NMR-oriented basis sets have a superior performance in the modern DFT calculations as compared to the usual energy-optimized basis sets. As an example, the pecS-*n* basis sets demonstrate particularly accurate results for the DFT calculations of NMR chemical shifts of a number of nuclei. In particular, the phosphorus NMR calculations are among the most challenging tasks, and the average absolute deviations of calculated theoretical values of ^{31}P NMR chemical shifts from experiment usually vary in the range of 7–9 ppm for the DFT-based schemes.[76–80] However, the use of the (aug-)pecG-2 basis set on phosphorus at the geometry optimization stage and (aug-)pecS-2 basis set for the NMR shielding calculation within the DFT-based computational protocols allows one to reduce this error to 4–5 ppm.[71,72,74]

4. Non-empirical NMR calculations

Principal results in this field were achieved by Stephan Sauer (University of Copenhagen) and his numerous collaborators and coauthors from all over the world. As an example, in the interim of 2020–2025, these authors published a series of papers dealing with the high-level non-empirical calculations of chemical shifts and indirect spin–spin coupling constants in the series of classical organic compounds,[81–83] fluorine-containing molecules,[84–86] and organometallic compounds.[52,87–91] Those studies were performed in parallel with a general development of NMR-oriented polarization propagator (PP) theory and higher-level methods[92–96] together with the high-level calculation of rovibrational corrections and solvent effects.[97]

The most popular approximation of PP theory is the Second-Order Polarization Propagator Approach known or SOPPA.[45,98–103] In the SOPPA method, the manifold is restricted to the subset of one- and two-electron excitations/de-excitations. The SOPPA method demonstrates a noticeable improvement in the accuracy of the calculations of both singlet and triplet NMR properties over the Random Phase Approximation (known as 'RPA') method. In addition, SOPPA method assumes a simple systematic extension to higher orders, implying a sequential improvement in the description of the electron correlation effects.

There are two basic modifications of the SOPPA method – SOPPA(CC2)[104] and SOPPA(CCSD).[105] These approximations were created to improve the accuracy of the calculation of spin–spin coupling constants relative to the original SOPPA method by replacing the Møller–Plesset perturbation coefficients with the coupled cluster amplitudes obtained from the corresponding coupled cluster scheme, which makes it imperative to solve the system of cluster equations. This essentially complicates calculations, and, in the case of the SOPPA(CCSD) scheme, even increases the scalability of the method up to N^6. However, the SOPPA method and its modifications have become very popular in the calculations of spin–spin coupling constants of various types.[45,49,101,106–108]

One of such examples is provided in Figure 21 adopted from the paper by Ukhanev *et al.*[109,110] In that study, all possible fluorine spin–spin coupling constants, ^{19}F–^{19}F, ^{19}F–^{13}C, and ^{19}F–^{1}H, of pentafluorobenzene were calculated at five different levels of theory, HF, DFT, SOPPA, CCSD, and the SOPPA(CCSD)-based composite scheme with taking into account solvent, vibrational, relativistic, and correlation corrections. Most corrections were next to negligible for the long-range couplings but quite essential for the one-bond carbon–fluorine coupling constants. Hartree–Fock calculations were found by the authors to be entirely unreliable, while DFT results were comparable in accuracy with the data obtained using the wave function-based methods. Based on those results, it was found that taking into account correlation, solvent, vibrational, and even relativistic corrections was highly recommended for the related studies, especially for the one-bond fluorine coupling constants.

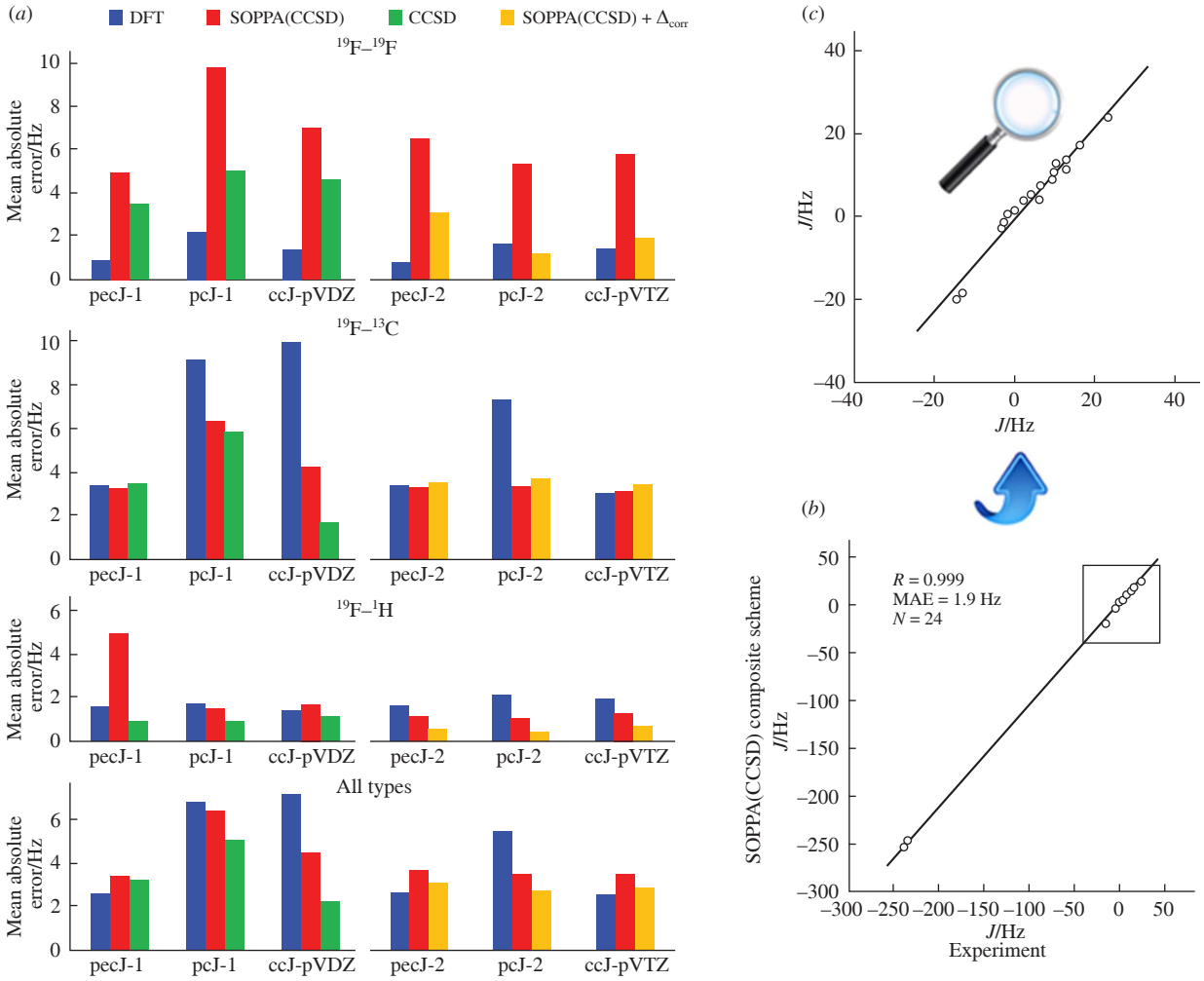


Figure 21 (*a*) Mean absolute errors of the correlations of $^{19}F–^{19}F$, $^{19}F–^{13}C$, and $^{19}F–^{1}H$ spin–spin coupling constants of pentafluorobenzene, calculated at different levels of theory, against experiment. (*b*) Correlation plot of calculated spin–spin coupling constants of all types in pentafluorobenzene. (*c*) Expanded range for geminal, vicinal, and longer-range couplings. Reproduced with minor editing privilege from Ukhanev *et al.*[110] with the permission of Elsevier.

In addition to the discussion of the polarization propagator approaches within the problem of NMR calculations, it is worth noting that there is another polarization propagator method, the so-called Algebraic Diagrammatic Construction (ADC)[111,112] and its second-order scheme, the ADC(2), which takes into account accordingly single and double excitations in the calculation of spin–spin coupling constants.[113] The formal operation cost of ADC is equivalent to that of the SOPPA method (N^5).

The other most popular *ab initio* approach extensively applied in the calculation of NMR parameters, is the Coupled Clusters (CC) method.[114–120] This method is one of the most accurate and reliable *ab initio* approaches, accounting for the electron correlation effects. The CC theory takes a special place in quantum chemistry, because it results in a hierarchy of approximate models, which provide a systematical convergence towards the full configuration interaction limit while maintaining the dimensional extensiveness at each hierarchical level.[21,122]

There are several very popular CC schemes, which are of the main interest for today. Among them is the Coupled Clusters Singles and Doubles (CCSD) model,[123] which arises from the sequential inclusion of single- and double-excitation operators in the major excitation operator. The next scheme is the coupled clusters singles, doubles and triples (CCSDT),[124–127] which adds to the consideration the triple excitations. The hierarchy continues up to CCSDTQ,[128–130] however, computational cost rapidly increases with each additional excitation class. In particular, the CCSD, CCSDT and CCSDTQ schemes have the scaling factors N^6, N^8, and N^9, respectively.[118,131] Notwithstanding the fact that CCSDT and CCSDTQ schemes are applicable in practice, these must be applicable only to very small systems (those like light di- and triatomics).

The CC3 model represents an intermediate case between the CCSD and CCSDT schemes, so that computational scalability of the former is N^7. In the CCSD(T) scheme, the triples amplitudes are estimated from the triples excitation equations as they occur in the lowest non-vanishing order for the Möller–Plesset perturbational theory. Overall, the CCSD(T) model has been proven successful and is used for accurate prediction of NMR properties. The scaling of the CCSD(T) scheme with respect to the number of basis sets functions is the same as that of the CC3 model, namely N^7. The coupled cluster methods are widely used nowadays to calculate NMR parameters of small and medium-sized molecular systems. Of all these models, the CCSD scheme turned out to be the most popular for calculating different types of spin–spin coupling constants.[132–136] The implementation of GIAO formalism to the CCSD(T) and CCSDT models was proposed by Auer, Gauss and Stanton[137] and Gauss[138] and was shown to be particularly effective in the calculation of NMR shielding constants.[139]

5. Conclusions

The development of NMR computational methods has come a long way from simulative and iterative codes like classical LAOCOON, VALISA, and PANIC to the high-level *ab initio* programs like non-relativistic GAMESS and Gaussian, two-component relativistic ADF and four-component relativistic

Dirac, which are based on a general Polarization Propagator approach and Coupled Cluster theory. Basically, four main stages in the development of NMR computational methods can be traced, they are (*a*) the creation of programs based on the simulation of NMR spectra within the framework of a spin Hamiltonian theory; (*b*) the appearance of semiempirical methods based on the full or intermediate neglect of differential overlap; (*c*) rapid penetration of the electron density functional theory (being something intermediate between semiempirical and *ab initio* methods) into the field of NMR calculations; and finally, (*d*) the establishment of purely *ab initio* NMR calculations within the framework of the Polarization Propagator theory and the Coupled Cluster Singles and Doubles (CCSD). Calculations of NMR parameters within the framework of the higher-level *ab initio* theory are not yet available at the current level of computational resources, however, with the exception of some particular cases.

To be more specific, several dozens of NMR simulative and iterative codes are and being used in NMR spectral analysis. Among them are those that were created for the iterative analysis of NMR strongly coupled spin systems, like classical LAOCOON, VALISA, and PANIC. A number of other less general codes like ANATOLIA, ANATOLIA-X, WinDNMR, NMR-SIM, DAISY, DAVINS, NMRCON, PERCHit, ChemAdder, NUTS, gNMR, MestRenova, SPINACH, and SpinWorks were also established and widely used in practical NMR spectral analysis.

At an early stage of the development of NMR computations, very popular were semiempirical methods like CNDO (Complete Neglect of Differential Overlap), INDO (Intermediate Neglect of Differential Overlap), MINDO (Modified Intermediate Neglect of Differential Overlap), MNDO (Modified Neglect of Diatomic Overlap), AM1 (Austin Model 1), and PM3 (Neglect of Differential Diatomic Overlap).

The DFT NMR-based computations became extremely popular in the recent years because they take into account electron correlation effects *via* the exchange–correlation potential requiring essentially low computational efforts. The main idea of the DFT methodology consists in using the electron density rather than a many-particle wavefunction (in contrast to the non-empirical methods) for describing a given electron system, which leads to a significant simplification of calculations and as a result, essential economy of computational efforts.

Non-empirical NMR calculations are mostly based on general Polarization Propagator theory implemented in the Second-Order Polarization Propagator Approach, SOPPA. The SOPPA method demonstrates a noticeable improvement in the accuracy of the calculations of both singlet and triplet NMR properties over the Random Phase Approximation. In addition, SOPPA method assumes a simple systematic extension to higher orders, implying a sequential improvement in the description of the electron correlation effects. In the SOPPA method, the manifold is restricted to the subset of one- and two-electron excitations/de-excitations. There are two basic modifications of this method – SOPPA(CC2) and SOPPA(CCSD). The coupled cluster methods are widely used nowadays to calculate NMR parameters of small and even medium-sized molecular systems. Of all these approaches, the CCSD scheme turned out to be the most popular and robust method for calculating NMR parameters.

References

1 L. B. Krivdin, *Mendeleev Commun.*, 2026, **36**, 245; https://doi.org/10.71267/mencom.8004.
2 I. L. Rusakova and L. B. Krivdin, *Int. Rev. Phys. Chem.*, 2023, **42**, 53; https://doi.org/10.1080/0144235X.2025.2529116.
3 L. B. Krivdin, *Int. Rev. Phys. Chem.*, 2025, **44**, 1; https://doi.org/10.1080/0144235X.2025.2572166.
4 I. L. Rusakova and L. B. Krivdin, in *NMR Spectroscopic Parameters: Theories and Models, Computational Codes and Calculations*, ed. G. A. Aucar (*New Developments in NMR*, vol. 38), Royal Society of Chemistry, 2025, pp. 1–61; https://doi.org/10.1039/9781837678020-00001.
5 E. Haapaniemi, *Magn. Reson. Chem.,* 2017, **55**, 804; https://doi.org/10.1002/mrc.4590.
6 S. V. Zubkov, S. S. Golotvin and V. A. Chertkov, *Russ. Chem. Bull.*, 2002, **51**, 1222; https://doi.org/1066-5285/02/5107-1222.
7 D. A. Cheshkov, K. F. Sheberstov, D. O. Sinitsyn and V. A. Chertkov, *Magn. Reson. Chem.*, 2018, **56**, 449; https://doi.org/10.1002/mrc.4689.
8 M. Edgar, F. Zeinali, M. Mojally, C. Hughes, S. Riaz and G. W. Weaver, *J. Fluorine Chem.*, 2019, **224**, 35; https://doi.org/10.1016/j.jfluchem.2019.04.018.
9 M. Edgar, D. Hayward, F. Zeinali, S. Riaz and G. W. Weaver, *Magn. Reson. Chem.*, 2020, **58**, 170; https://doi.org/10.1002/mrc.4947.
10 A. I. Nichugovskiy, V. V. Zamalyutin, V. R. Flid and D. A. Cheshkov, *Magn. Reson. Chem.*, 2026, **64**, 690; https://doi.org/10.1002/mrc.70111.
11 D. A. Cheshkov and D. O. Sinitsyn, *Magn. Reson.*, 2026, **7**, 15; https://doi.org/10.5194/mr-7-15-2026.
12 L. B. Krivdin, *NMR Spectroscopy of Unsaturated Heteroatomic Compounds*, *PhD Thesis*, Irkutsk, 1982, reg. no. 04820018864.
13 J. R. Sabin, D. P. Santry and K. Weiss, *J. Am. Chem. Soc.*, 1972, **94**, 6651; https://doi.org/10.1021/ja00774a014.
14 L. A. Carreira and W. B. Person, *J. Am. Chem. Soc.*, 1972, **94**, 1485; https://doi.org/10.1021/ja00760a010.
15 M. J. S. Dewar and E. Haselbach, *J. Am. Chem. Soc.*, 1970, **92**, 590; https://doi.org/10.1021/ja00706a029.
16 M. J. S. Dewar and W. Thiel, *J. Am. Chem. Soc.*, 1977, **99** 4899; https://doi.org/10.1021/ja00457a004.
17 M. J. S. Dewar, E. G. Zoebisch, E. F. Healy and J. J. P. Stewart, *J. Am. Chem. Soc.*, 1985, **107**, 3902; https://doi.org/10.1021/ja00065a080.
18 J. J. P. Stewart, *J. Comput. Chem.*, 1989, **10**, 209; https://doi.org/10.1002/jcc.540100208.
19 V. G. Malkin, O. L. Malkina and D. R. Salahub, *Chem. Phys. Lett.*, 1993, **204**, 80; https://doi.org/10.1016/0009-2614(93)85608-Q.
20 V. G. Malkin, O. L. Malkina, M. E. Casida and D. R. Salahub, *J. Am. Chem. Soc.*, 1994, **116**, 5898; https://doi.org/10.1021/ja00092a046.
21 V. G. Malkin, O. L. Malkina and D. R. Salahub, *Chem. Phys. Lett.*, 1993, **204**, 87; https://doi.org/10.1016/0009-2614(93)85609-R.
22 W. Kutzelnigg, U. Fleischer and M. Schindler, in *Deuterium and Shift Calculation*, eds. P. Diehl, E. Fluck, H. Günther, R. Kosfeld and J. Seelig *(NMR Basic Principles and Progress*, vol. 23), Springer, Berlin, 1990, pp. 165–262; https://doi.org/10.1007/978-3-642-75932-1.
23 G. Schreckenbach and T. Ziegler, *J. Phys. Chem.*, 1995, **99**, 606; https://doi.org/10.1021/j100002a024.
24 G. Schreckenbach and T. Ziegler, *Int. J. Quant. Chem.*, 1996, **60**, 753; https://doi.org/10.1002/(SICI)1097-461X(1996)60:3<753::AID-QUA4>3.0.CO;2-W.
25 G. Schreckenbach, R. M. Dickson, Y. Ruiz–Morales and T. Ziegler, in *Chemical Applications of Density-Functional Theory (ACS Symposium Series*, vol. 629), eds. B. B. Laird, R. B. Ross and T. Ziegler, American Chemical Society, Washington, 1996, ch. 23, pp. 328–341; https://doi.org/10.1021/bk-1996-0629.ch023.
26 G. Schreckenbach and T. Ziegler, *Int. J. Quantum Chem.*, 1997, **61**, 899; https://doi.org/10.1002/(SICI)1097-461X(1997)61:6<899::AID-QUA3>3.0.CO;2-R.
27 G. Schreckenbach and T. Ziegler, *Theor. Chem. Acc.*, 1998, **99**, 71; https://doi.org/10.1007/s002140050306.
28 K. Wolinski, J. F. Hinton and P. Pulay, *J. Am. Chem. Soc.*, 1990, **112**, 8251; https://doi.org/10.1021/ja00179a005.
29 R. Ditchfield, *J. Chem. Phys.*, 1972, **56**, 5688; https://doi.org/10.1063/1.1677088.
30 G. Rauhut, S. Puyear, K. Wolinski and P. Pulay, *J. Phys. Chem.*, 1996, **100**, 6310; https://doi.org/10.1021/jp9529127.
31 J. R. Cheeseman, G. W. Trucks, T. A. Keith and M. J. Frisch, *J. Chem. Phys.*, 1996, **104**, 5497; https://doi.org/10.1063/1.471789.
32 A. M. Lee, N. C. Handy and S. M. Colwell, *J. Chem. Phys.*, 1995, **103**, 10095; https://doi.org/10.1063/1.469912.
33 L. Olsson and D. Cremer, *J. Chem. Phys.*, 1996, **105**, 8995; https://doi.org/10.1063/1.472729.
34 M. E. Harding, M. Lenhart, A. A. Auer and J. Gauss, *J. Chem. Phys.*, 2008, **128**, 244111; https://doi.org/10.1063/1.2943145.
35 A. M. Teale, O. B. Lutnæs, T. Helgaker, D. J. Tozer and J. Gauss, *J. Chem. Phys.*, 2013, **138**, 024111; https://doi.org/10.1063/1.4773016.

36 E. Fadda, M. E. Casida and D. R. Salahub, *Int. J. Quantum Chem.*, 2003, **91**, 67; https://doi.org/10.1002/qua.10434.
37 D. Xin, C. A. Sader, O. Chaudhary, P.–J. Jones, K. Wagner, C. S. Tautermann, Z. Yang, C. A. Busacca, R. A. Saraceno, K. R. Fandrick, N. C. Gonnella, K. Horspool, G. Hansen and C. H. Senanayake, *J. Org. Chem.*, 2017, **82**, 5135; https://doi.org/10.1021/acs.joc.7b00321.
38 M. Alipour, *RSC Adv.*, 2015, **5**, 4737; https://doi.org/10.1039/c4ra13186j.
39 T. W. Keal and D. J. Tozer, *J. Chem. Phys.*, 2003, **119**, 3015; https://doi.org/10.1063/1.1590634.
40 T. W. Keal and D. J. Tozer, *J. Chem. Phys.*, 2004, **121**, 5654; https://doi.org/10.1063/1.1784777.
41 S. L. V. Zahn, O. Hammerich, P. E. Hansen and S. P. A. Sauer, *J. Comput. Chem.*, 2021, **42**, 1248; https://doi.org/10.1002/jcc.26540.
42 G. L. Stoychev, A. A. Auer and F. Neese, *J. Chem. Theory Comput.*, 2018, **14**, 4756; https://doi.org/10.1021/acs.jctc.8b00624.
43 G. Saielli, *Magn. Reson. Chem.*, 2020, **58**, 548; https://doi.org/10.1002/mrc.4962.
44 F. Reviriego, E. Peña–Cabrera, S. V. Kokate, I. Alkorta and J. Elguero, *Magn. Reson. Chem.*, 2021, **59**, 454; https://doi.org/10.1002/mrc.5118.
45 T. Enevoldsen, J. Oddershede and S. P. A. Sauer, *Theor. Chim. Acta*, 1998, **100**, 275; https://doi.org/10.1007/s002140050388.
46 P. F. Provasi, G. A. Aucar and S. P. A. Sauer, *J. Chem. Phys.*, 2001, **115**, 1324; https://doi.org/10.1063/1.1379331.
47 P. F. Provasi and S. P. A. Sauer, *J. Chem. Phys.*, 2010, **133**, 054308; https://doi.org/10.1063/1.3465553.
48 V. Barone, P. F. Provasi, J. E. Peralta, J. P. Snyder, S. P. A. Sauer and R. H. Contreras, *J. Phys. Chem. A*, 2003, **107**, 4748; https://doi.org/10.1021/jp0300851.
49 S. P. A. Sauer, W. T. Raynes and R. A. Nicholls, *J. Chem. Phys.*, 2001, **115**, 5994; https://doi.org/10.1063/1.1398091.
50 P. Lazzeretti, M. Malagoli and R. Zanasi, *Chem. Phys. Lett.*, 1994, **220**, 299; https://doi.org/10.1016/0009-2614(94)00158-8.
51 E. D. Hedegård, J. Kongsted and S. P. A. Sauer, *J. Chem. Theory Comput.*, 2011, **7**, 4077; https://doi.org/10.1021/ct200587k.
52 C. Steinmann and S. P. A. Sauer, *Magn. Reson. Chem.*, 2021, **59**, 1134; https://doi.org/10.1002/mrc.5166.
53 F. Jensen, *J. Chem. Theory Comput.*, 2006, **2**, 1360; https://doi.org/10.1021/ct600166u.
54 F. Jensen, *Theor. Chim. Acta*, 2010, **126**, 371; https://doi.org/10.1007/s00214-009-0699-5.
55 P. A. Aggelund, S. P. A. Sauer and F. Jensen, *J. Chem. Phys.*, 2018, **149**, 044117; https://doi.org/10.1063/1.5034109.
56 F. Jensen, *J. Chem. Phys.*, 2001, **115**, 9113; https://doi.org/10.1063/1.1413524.
57 F. Jensen, *J. Chem. Phys.*, 2002, **116**, 7372; https://doi.org/10.1063/1.1465405.
58 F. Jensen and T. Helgaker, *J. Chem. Phys.*, 2004, **121**, 3463; https://doi.org/10.1063/1.1756866.
59 F. Jensen, *J. Chem. Phys.*, 2007, **111**, 11198; https://doi.org/10.1021/jp068677h.
60 F. Jensen, *J. Chem. Phys.*, 2002, **117**, 9234; https://doi.org/10.1063/1.1515484.
61 Yu. Yu. Rusakov and I. L. Rusakova, *J. Phys. Chem. A*, 2019, **123**, 6564; https://doi.org/10.1021/acs.jpca.9b05276.
62 Yu. Yu. Rusakov and I. L. Rusakova, *Magn. Reson. Chem.*, 2021, **59**, 713; https://doi.org/10.1002/mrc.5132.
63 Yu. Yu. Rusakov and I. L. Rusakova, *Phys. Chem. Chem. Phys.*, 2021, **23**, 14925; https://doi.org/10.1039/d1cp01984h.
64 Yu. Yu. Rusakov and I. L. Rusakova, *Molecules*, 2021, **27**, 6145; https://doi.org/10.3390/molecules27196145.
65 Yu. Yu. Rusakov and I. L. Rusakova, *Int. J. Mol. Sci.*, 2023, **24**, 7841; https://doi.org/10.3390/ijms24097841.
66 F. Jensen, *J. Chem. Theory Comput.*, 2015, **11**, 132; https://doi.org/10.1021/ct5009526.
67 Y. J. Franzke, R. Treß, T. M. Pazdera and F. Weigend, *Phys. Chem. Chem. Phys.*, 2019, **21**, 16658; https://doi.org/10.1039/c9cp02382h.
68 Yu. Yu. Rusakov and I. L. Rusakova, *J. Chem. Phys.*, 2022, **156**, 244112; https://doi.org/10.1063/5.0096907.
69 Yu. Yu. Rusakov and I. L. Rusakova, *J. Chem. Phys.*, 2025, **162**, 164111; https://doi.org/10.1063/5.0265111.
70 Yu. Yu. Rusakov, V. A. Semenov and I. L. Rusakova, *Int. J. Mol. Sci.*, 2023, **24**, 14623; https://doi.org/10.3390/ijms241914623.
71 Yu. Yu. Rusakov and I. L. Rusakova, *Phys. Chem. Chem. Phys.*, 2023, **25**, 18728; https://doi.org/10.1039/d3cp02664g.
72 Yu. Yu. Rusakov, Yu. A. Nikurashina and I. L. Rusakova, *Phys. Chem. Chem. Phys.*, 2025, **27**, 6730; https://doi.org/10.1039/d5cp00313j.
73 Yu. Yu. Rusakov and I. L. Rusakova, *J. Chem. Theory Comput.*, 2024, **20**, 6661; https://doi.org/10.1021/acs.jctc.4c00772.s001.
74 Yu. Yu. Rusakov, Yu. A. Nikurashina and I. L. Rusakova, *J. Chem. Phys.*, 2024, **160**, 084109; https://doi.org/10.1063/5.0193227.
75 Yu. Yu. Rusakov, V. A. Semenov and I. L. Rusakova, *Int. J. Mol. Sci.*, 2024, **25**, 10588; https://doi.org/10.3390/ijms251910588.
76 S. V. Fedorov, Yu. Yu. Rusakov and L. B. Krivdin, *Magn. Reson. Chem.*, 2014, **52**, 699; https://doi.org/10.1002/mrc.4122.
77 S. K. Latypov, F. M. Polyancev, D. G. Yakhvarov and O. G. Sinyashin, *Phys. Chem. Chem. Phys.*, 2015, **17**, 6976; https://doi.org/10.1039/c5cp00240k.
78 S. K. Latypov, S. A. Kondrashova, F. M. Polyancev and O. G. Sinyashin, *Organometallics*, 2020, **39**, 1413; https://doi.org/10.1021/acs.organomet.0c00127.
79 S. A. Kondrashova, F. M. Polyancev and S. K. Latypov, *Molecules*, 2022, **27**, 2668; https://doi.org/10.3390/molecules27092668.
80 W. H. Hersh and T.-Y. Chan, *Beilstein J. Org.Chem.*, 2023, **19**, 36; https://doi.org/10.3762/bjoc.19.4.
81 M. N. C. Zarycz, P. F. Provasi, M. M. Vallejos and S. P. A. Sauer, *Trends Phys. Chem.*, 2021, **21**, 41; https://researchprofiles.ku.dk/en/publications/indirect-nuclear-spin-spin-coupling-constants-and-chemical-shifts/.
82 C. H. S. Møller, A. K. Schnack-Petersen and S. P. A. Sauer, *Mol. Phys.*, 2020, **118**, e1757773; https://doi.org/10.1080/00268976.2020.1757773.
83 H. Moustafa, F. H. Larsen, A. Ø. Madsen and S. P. A. Sauer, *Magnetochemistry*, 2023, **9**, 192; https://doi.org/10.3390/magnetochemistry9080192.
84 M. de Giovanetti, R. Cormanich and S. P. A. Sauer, *J. Chem. Theory Comput.*, 2024, **20**, 10453; https://doi.org/10.1021/acs.jctc.4c01043.
85 M. de Giovanetti, L. F. F. Bitencourt, R. Cormanich and S. P. A. Sauer, *J. Chem. Theory Comput.*, 2021, **17**, 7712; https://doi.org/10.1021/acs.jctc.1c00287.
86 M. Jaszunski, S. P. A. Sauer, R. Faber and D. J. D. Wilson, *Phys. Chem. Chem. Phys.*, 2020, **22**, 21350; https://doi.org/10.1039/d0cp02730h.
87 L. M. Jessen, S. P. A. Sauer and L. B. S. Hemmingsen, *Inorg. Chem.*, 2024, **63**, 23614; https://doi.org/10.1021/acs.inorgchem.4c03518.
88 H. Wu, L. B. S. Hemmingsen and S. P. A. Sauer, *Magn. Reson. Chem.*, 2024, **62**, 648; https://doi.org/10.1002/mrc.5452.
89 J. B. Dos R. Lino, M. A. Gonçalves, S. P. A. Sauer and T. C. Ramalho, *Magnetochemistry*, 2022, **8**, 47; https://doi.org/10.3390/magnetochemistry8050047.
90 I. Glent-Madsen, A. Reinholdt, J. Bendix and S. P. A. Sauer, *Organometallics*, 2021, **40**, 1443; https://doi.org/10.1021/acs.organomet.1c00079.
91 J. B. Dos R. Lino, S. P. A. Sauer and T. C. Ramalho, *J. Phys. Chem. A*, 2020, **124**, 4946; https://doi.org/10.1021/acs.jpca.0c01607.
92 C. H. S. Møller and S. P. A. Sauer, *Magn. Reson. Chem.*, 2025, **63**, 328; https://doi.org/10.1002/mrc.5514.
93 L. M. Jessen and S. P. A. Sauer, *J. Chem. Phys.*, 2024, **160**, 064102; https://doi.org/10.1063/5.0189932.
94 J. S. Rodrigo, A. E. Hillers-Bendtsen, F. Ø. Kjeldal, N. M. Høyer, K. V. Mikkelsen and S. P. A. Sauer, *J. Chem. Phys.*, 2023, **158**, 124118; https://doi.org/10.1063/5.0140117.
95 A. K. Schnack-Petersen, M. Simmermacher, E. Fasshauer, H. J. A. Jensen and S. P. A. Sauer, *J. Chem. Phys.*, 2020, **152**, 134113; https://doi.org/10.1063/5.0002389.
96 R. Faber, S. P. A. Sauer and J. Gauss, *J. Chem. Theory Comput.*, 2017, **13**, 696; https://doi.org/10.1021/acs.jctc.6b01003.
97 L. M. Jessen, P. Reinholdt, J. Kongsted and S. P. A. Sauer, *Magnetochemistry*, 2023, **9**, 102; https://doi.org/10.3390/magnetochemistry9040102.
98 J. Oddershede, in *Methods in Computational Molecular Physics*, eds. S. Wilson and G. H. F. Diercksen (*NATO ASI Series*, vol. 293), Springer, Boston, MA, 1992, pp. 303–324; https://doi.org/10.1007/978-1-4615-7419-4_12.
99 R. D. Wigglesworth, W. T. Raynes, S. P. A. Sauer and J. Oddershede, *Mol. Phys.*, 1997, **92**, 77; https://doi.org/10.1080/002689797170635.
100 R. D. Wigglesworth, W. T. Raynes, S. P. A. Sauer and J. Oddershede, *Mol. Phys.*, 1998, **94**, 851; https://doi.org/10.1080/002689798167700.
101 R. D. Wigglesworth, W. T. Raynes, S. Kirpekar, J. Oddershede and S. P. A. Sauer, *J. Chem. Phys.*, 2000, **112**, 3735; https://doi.org/10.1063/1.480525.
102 E. S. Nielsen, P. Jørgensen and J. Oddershede, *J. Chem. Phys.*, 1980, **73**, 6238; https://doi.org/10.1063/1.440119.
103 K. L. Bak, H. Koch, J. Oddershede, O. Christiansen and S. P. A. Sauer, *J. Chem. Phys.*, 2000, **112**, 4173; https://doi.org/10.1063/1.480963.
104 H. Kjær, S. P. A. Sauer and J. Kongsted, *J. Chem. Phys.*, 2010, **133**, 144106; https://doi.org/10.1063/1.3483197.

105 S. P. A. Sauer, *J. Phys. B: At. Mol. Opt. Phys.*, 1997, **30**, 3773; https://doi.org/10.1088/0953-4075/30/17/007.
106 S. P. A. Sauer and W. T. Raynes, *J. Chem. Phys.*, 2000, **113**, 3121; https://doi.org/10.1063/1.1287277.
107 P. F. Provasi, G. A. Aucar and S. P. A. Sauer, *J. Chem. Phys.*, 2000, **112**, 6201; https://doi.org/10.1063/1.481219.
108 S. P. A. Sauer, I. Paidarová and J. Oddershede, *Theor. Chim. Acta*, 1994, **88**, 351; https://doi.org/10.1007/BF01113553.
109 S. A. Ukhanev, S. V. Fedorov, Y. Y. Rusakov, I. L. Rusakova and L. B. Krivdin, *Magn. Reson. Chem.*, 2022, **60**, 901; https://doi.org/10.1002/mrc.5276.
110 S. A. Ukhanev, S. V. Fedorov, Y. Y. Rusakov, I. L. Rusakova and L. B. Krivdin, *J. Fluorine Chem.*, 2023, **266**, 110093; https://doi.org/10.1016/j.jfluchem.2023.110093.
111 J. Schirmer, *Phys. Rev. A*, 1982, **26**, 2395; https://doi.org/10.1103/PhysRevA.26.2395.
112 A. B. Trofimov, I. L. Krivdina, J. Weller and J. Schirmer, *Chem. Phys.*, 2006, **329**, 1; https://doi.org/10.1016/j.chemphys.2006.07.015.
113 I. L. Rusakova, L. B. Krivdin, Yu. Yu. Rusakov and A. B. Trofimov, *J. Chem. Phys.*, 2012, **137**, 044119; https://doi.org/10.1063/1.4737181.
114 H. J. Monkhorst, *Int. J. Quantum Chem., Symp.*, 1977, **12**, 421; https://doi.org/10.1002/qua.560120850.
115 R. J. Bartlett and M. Musiał, *Rev. Mod. Phys.*, 2007, **79**, 291; https://doi.org/10.1103/RevModPhys.79.291.
116 H. Koch and P. Jørgensen, *J. Chem. Phys.*, 1990, **93**, 3333; https://doi.org/10.1063/1.458814.
117 R. J. Bartlett and G. D. Purvis III, *Phys. Scripta*, 1980, **21**, 255; https://doi.org/10.1088/0031-8949/21/3-4/007.
118 O. Christiansen, *Theor. Chim. Acta*, 2006, **116**, 106; https://doi.org/10.1007/s00214-005-0037-5.
119 J. Paldus, P. E. S. Wormer, F. Visser and A. van der Avoird, *J. Chem. Phys.*, 1982, **76**, 2458; https://doi.org/10.1063/1.443275.
120 H. Koch, A. Sánchez de Merás, T. Helgaker and O. Christiansen, *J. Chem. Phys.*, 1996, **104**, 4157; https://doi.org/10.1063/1.471227.
121 T. Helgaker, S. Coriani, P. Jørgensen, K. Kristensen, J. Olsen and K. Ruud, *Chem. Rev.*, 2012, **112**, 543; https://doi.org/10.1021/cr2002239.
122 J. Gauss and J. F. Stanton, in *Calculation of NMR and EPR Parameters. Theory and Applications*, eds. M. Kaupp, M. Bühl and V. G. Malkin, Wiley–VCH, Weinheim, 2004, ch. 8, pp. 123–139; https://doi.org/10.1002/3527601678.
123 G. E. Scuseria, C. L. Janssen and H. F. Schaefer, *J. Chem. Phys.*, 1988, **89**, 7382; https://doi.org/10.1063/1.455269.
124 Y. S. Lee, S. A. Kucharski and R. J. Bartlett, *J. Chem. Phys.*, 1984, **81**, 5906; https://doi.org/10.1063/1.447591.
125 G. E. Scuseria and H. F. Schaefer III, *Chem. Phys. Lett.*, 1988, **152**, 382; https://doi.org/10.1016/0009-2614(88)80110-6.
126 M. Urban, J. Noga, S. J. Cole and R. J. Bartlett, *J. Chem. Phys.*, 1985, **83**, 4041; https://doi.org/10.1063/1.449067.
127 J. Noga, R. J. Bartlett and M. Urban, *Chem. Phys. Lett.*, 1987, **134**, 126; https://doi.org/10.1016/0009-2614(87)87107-5.
128 S. A. Kucharski and R. J. Bartlett, *J. Chem. Phys.*, 1992, **97**, 4282; https://doi.org/10.1063/1.463930.
129 N. Oliphant and L. Adamowicz, *J. Chem. Phys.*, 1991, **95**, 6645; https://doi.org/10.1063/1.461534.
130 S. A. Kucharski and R. J. Bartlett, *Theor. Chim. Acta*, 1991, **80**, 387; https://doi.org/10.1007/BF01117419.
131 D. A. Matthews, *Mol. Phys.*, 2020, **118**, e1757774; https://doi.org/10.1021/ct800111j.
132 M. Pecul and T. Helgaker, *Int. J. Mol. Sci.*, 2003, **4**, 143; https://doi.org/10.3390/i4030143.
133 S. A. Perera, H. Sekino and R. J. Bartlett, *J. Chem. Phys.*, 1994, **101**, 2186; https://doi.org/10.1063/1.467725.
134 J. E. Del Bene, I. Alkorta and J. Elguero, *J. Chem. Theory Comput.*, 2009, **5**, 208; https://doi.org/10.1021/ct800321b.
135 J. E. Del Bene, I. Alkorta and J. Elguero, *J. Phys. Chem. A*, 2009, **113**, 12411; https://doi.org/10.1021/jp902089g.
136 R. Faber and S. P. A. Sauer, *Theor. Chim. Acta*, 2018, **137**, 35; https://doi.org/10.1007/s00214-018-2217-0.
137 A. A. Auer, J. Gauss and J. F. Stanton, *J. Chem. Phys.*, 2003, **118**, 10407; https://doi.org/10.1063/1.1574314.
138 J. Gauss, *J. Chem. Phys.*, 2002, **116**, 4773; https://doi.org/10.1063/1.1462612.
139 D. Sundholm, J. Gauss and A. Schäfer, *J. Chem. Phys.*, 1996, **105**, 11051; https://doi.org/10.1063/1.472905.

Received: 3rd August 2026; Com. 26/8166

Contents entry

Computational methods in the NMR spectral analysis: from early semiempirical simulations to modern *ab initio* calculations

Leonid B. Krivdin

